



Title	A Novel Combination of Prion Strain Co-Occurrence in Patients with Sporadic Creutzfeldt-Jakob Disease
Author(s)	Kobayashi, Atsushi; Iwasaki, Yasushi; Takao, Masaki; Saito, Yuko; Iwaki, Toru; Qi, Zechen; Torimoto, Ryouta; Shimazaki, Taishi; Munesue, Yoshiko; Isoda, Norikazu; Sawa, Hirofumi; Aoshima, Keisuke; Kimura, Takashi; Kondo, Hinako; Mohri, Shirou; Kitamoto, Tetsuyuki
Citation	The American Journal of Pathology, 189(6), 1276-1283 https://doi.org/10.1016/j.ajpath.2019.02.012
Issue Date	2019-06
Doc URL	http://hdl.handle.net/2115/78372
Rights	© 2019, Elsevier. Licensed under the Creative Commons Attribution-NonCommercial-NoDerivatives 4.0 International http://creativecommons.org/licenses/by-nc-nd/4.0/
Rights(URL)	https://creativecommons.org/licenses/by-nc-nd/4.0/
Type	article (author version)
File Information	The American Journal of Pathology189(6)_1276-1283.pdf



[Instructions for use](#)

1 **Title:** A novel combination of prion strain co-occurrence in patients with sporadic
2 Creutzfeldt-Jakob disease

3

4 **Authors:** Atsushi Kobayashi,^{1*} Yasushi Iwasaki,² Masaki Takao,³ Yuko Saito,⁴ Toru
5 Iwaki,⁵ Zechen Qi,¹ Ryouta Torimoto,¹ Taishi Shimazaki,¹ Yoshiko Munesue,¹
6 Norikazu Isoda,^{6,7} Hirofumi Sawa,^{6,8} Keisuke Aoshima,¹ Takashi Kimura,¹ Hinako
7 Kondo,⁹ Shirou Mohri,⁹ Tetsuyuki Kitamoto⁹

8

9 **Affiliations:** ¹Laboratory of Comparative Pathology, Faculty of Veterinary Medicine,
10 Hokkaido University, Kita 18 Nishi 9, Kita-ku, Sapporo, 060-0818, Japan; ²Department
11 of Neuropathology, Institute for Medical Science of Ageing, Aichi Medical University,
12 1-1 Yazakokarimata, Nagakute, Aichi, 480-1195, Japan; ³Department of Neurology,
13 Saitama Medical University International Medical Center, 1397-1 Yamane, Hidaka,
14 Saitama, 350-1241, Japan; ⁴Department of Laboratory Medicine, National Center of
15 Neurology and Psychiatry Hospital, 4-1-1 Ogawa-higashi-machi, Kodaira, 187-8511,
16 Japan; ⁵Department of Neuropathology, Graduate School of Medical Sciences, Kyushu
17 University, 3-1-1 Maidashi, Higashi-ku, Fukuoka, 812-8582, Japan; ⁶Global Station for
18 Zoonosis Control, Global Institute for Collaborative Research and Education
19 (GI-CoRE), Hokkaido University; ⁷Unit of Risk Analysis and Management, Research
20 Center for Zoonosis Control, Hokkaido University, Kita 20 Nishi 10, Kita-ku, Sapporo,
21 001-0020, Japan; ⁸Division of Molecular Pathobiology, Research Center for Zoonosis
22 Control, Hokkaido University, Kita 20 Nishi 10, Kita-ku, Sapporo, 001-0020, Japan;
23 ⁹Department of Neurological Science, Tohoku University Graduate School of Medicine,
24 2-1 Seiryō-machi, Aoba-ku, Sendai, 980-8575, Japan

25

26 ***Corresponding author:** Atsushi Kobayashi; Laboratory of Comparative Pathology,
27 Faculty of Veterinary Medicine, Hokkaido University, Kita 18 Nishi 9, Kita-ku,
28 Sapporo, 060-0818, JAPAN; Tel, +81-11-706-5192; Fax, +81-11-706-5194; E-mail,
29 kobayashi@vetmed.hokudai.ac.jp

30

31 **Running head:** Co-occurrence of prion strains in sCJD

32

33 **Sources of support:** This study was supported by JSPS KAKENHI Grant Number
34 18K05963 (A.K.) and 18K06506 (M.T.), a grant from The Ichiro Kanehara Foundation
35 (A.K.), a grant from The Suhara Memorial Foundation (A.K.), a grant from The Kato
36 Memorial Trust for Nambyo Research (A.K.), Research Committee of Prion Disease
37 and Slow Virus Infection, Research on Policy Planning and Evaluation for Rare and
38 Intractable Diseases, Health and Labour Sciences Research Grants, The Ministry of
39 Health, Labour and Welfare, Japan (M.T.), and AMED under Grant Number
40 JP18dm0107103 (Y.S.).

41

42 **Disclosures:** None declared.

43

44 **Number of words in abstract:** 203

45 **Number of words in main text:** 2,909

46 **Number of figures (color figures):** 6 (3)

47 **Number of tables:** 1

48 **Number of supplemental materials:** 2

49

50 **Abstract**

51 Six subgroups of sporadic Creutzfeldt-Jakob disease have been identified by distinctive
52 clinicopathological features, genotype at polymorphic codon 129 (methionine/valine,
53 M/V) of the *PRNP* gene, and type of abnormal prion proteins (type 1 or 2). In addition
54 to the pure subgroups, mixed neuropathological features and co-existence of two types
55 of abnormal prion proteins in the same patient have also been reported. Here, we found
56 that a portion of the patients previously diagnosed as MM1 had neuropathological
57 characteristics of MM2 thalamic form, *i.e.*, neuronal loss of the inferior olivary nucleus
58 of the medulla. Furthermore, co-existence of biochemical features of MM2 thalamic
59 form was also confirmed in the identified cases. In addition, in transmission
60 experiments using prion protein-humanized mice, the brain material from the identified
61 case showed weak infectivity and generated characteristic abnormal prion proteins in
62 the inoculated mice resembling those after inoculation with a brain material of MM2
63 thalamic form. Taken together, these results show that the co-occurrence of MM1 and
64 MM2 thalamic form is a novel entity of sporadic Creutzfeldt-Jakob disease prion strain
65 co-occurrence. The present study raises the possibility that the co-occurrence of MM2
66 thalamic form might have been overlooked so far due to scarcity of abnormal prion
67 protein accumulation and restricted neuropathology.

68 **Introduction**

69 Prion diseases are lethal transmissible neurodegenerative diseases including
70 Creutzfeldt-Jakob disease (CJD), Gerstmann-Sträussler-Scheinker syndrome, fatal
71 familial insomnia (FFI), and variably protease-sensitive prionopathy in humans, or
72 scrapie, bovine spongiform encephalopathy, and chronic wasting disease in animals.
73 The central event in the pathogenesis of prion diseases is a conformational conversion
74 of the normal cellular isoform of prion protein (PrP^{C}) into an abnormal misfolded
75 isoform (PrP^{Sc}), which is a component of a proteinaceous infectious particle, namely
76 prion (1). The conformational conversion of PrP^{C} can occur due to either one of three
77 causes: [1] spontaneous conversion in sporadic CJD (sCJD) and variably
78 protease-sensitive prionopathy, [2] pathogenic mutations of the *PRNP* gene in genetic
79 CJD (gCJD), Gerstmann-Sträussler-Scheinker syndrome, and FFI, or [3] prion infection
80 in acquired prion diseases such as iatrogenic CJD, kuru, variant CJD (vCJD), scrapie,
81 bovine spongiform encephalopathy, and chronic wasting disease (2).

82 Patients with sCJD show clinical and neuropathological heterogeneity
83 associated with the genotype (methionine (M) or valine (V)) at polymorphic codon 129
84 of the *PRNP* gene and the type (1 or 2) of PrP^{Sc} accumulating in the brain (3). The types
85 1 and 2 PrP^{Sc} can be distinguished by the size of proteinase K-resistant core of the
86 protein (21 and 19 kDa, respectively) (3, 4). Based on these two determinants, sCJD
87 patients are currently classified into six subgroups: MM/MV1, MM2 cortical form
88 (MM2C), MM2 thalamic form (MM2T), VV1, VV2, and MV2 (5). The MM1 and MV1
89 subgroups are merged into one subgroup as MM/MV1 because they are
90 indistinguishable in clinicopathological and biochemical features (3). On the other hand,
91 the MM2 subgroup is further divided into two subgroups, MM2C and MM2T, because

92 they show distinctive neuropathological features (3). Widespread confluent vacuoles
93 and intense perivacuolar PrP deposition in the cerebral cortices are characteristics of
94 MM2C patients. By contrast, in MM2T patients, neuronal loss and gliosis are restricted
95 within thalamic nuclei and the inferior olivary nucleus of the medulla, and PrP
96 deposition is faint or negative. Transmission properties of the six sCJD subgroups have
97 also been examined systematically, and five prion strains have been recognized based
98 on the distinctive transmission properties, namely M1 (sCJD-MM/MV1), M2C
99 (sCJD-MM2C), M2T (sCJD-MM2T), V1 (sCJD-VV1), or V2 (sCJD-VV2 and -MV2)
100 strain (6, 7).

101 Co-occurrence of prion strains in the same brain is possible and results in the
102 presentation of mixed neuropathological features and more than one PrP^{Sc} type (3, 8-12).
103 The most frequently observed mixed subgroup is co-occurrence of M1 and M2C prion
104 strains, *i.e.*, sCJD-MM/MV1+2C, which accounts for 26% of total sCJD cases (12). The
105 sCJD-MM/MV1+2C patients show neuropathological and biochemical features of
106 sCJD-MM/MV2C, *i.e.*, confluent vacuoles, perivacuolar PrP deposition, and type 2
107 PrP^{Sc} accumulation, besides sCJD-MM/MV1 characteristics. Moreover, co-existing
108 M2C prion strain can affect the clinical features of patients as well as neuropathological
109 and biochemical properties, and the duration of illness becomes longer with increasing
110 M2C prion strain load (11, 12). However, co-existing M2C prion strain does not affect
111 the transmission properties because the infectivity of M2C strain is very low (13).

112 The relatively high incidence of co-occurrence of M1 and M2C strains
113 prompted us to investigate the possibility of other combinations of sCJD prion strain
114 co-occurrence. To date, co-occurrence of V1 and V2 strains, M2C and V2 strains, M1
115 and V2 strains, or M2C and M2T strains has been reported though the incidence rates

116 are very low (12). In the present study, we have demonstrated that a portion of sCJD
117 cases previously diagnosed as MM1 had neuropathological characteristics of
118 sCJD-MM2T. Furthermore, co-existence of biochemical properties of sCJD-MM2T was
119 also confirmed in the identified cases. The present study suggests that the co-occurrence
120 of M1 and M2T prion strains may also occur with a relatively high incidence rate.

121

122 **Materials and methods**

123 **Ethics statement**

124 This study was approved by the Institutional Ethics Committee of Hokkaido University
125 Graduate School of Veterinary Medicine (VET27-1). All experiments using human
126 materials were in compliance with the Helsinki Declaration. Animal experiments were
127 performed in strict accordance with the Regulations for Animal Experiments and
128 Related Activities at Hokkaido University and Fundamental Guidelines for Proper
129 Conduct of Animal Experiment and Related Activities in Academic Research
130 Institutions by Ministry of Education, Culture, Sports, Science and Technology in Japan,
131 Notice No. 71. The protocol was approved by the Institutional Animal Care and Use
132 Committees of Hokkaido University (14-0170).

133

134 **Patients**

135 CJD cases included in this study were patients with clinically, genetically and
136 histopathologically proven sCJD, gCJD, and FFI. Brain tissues were obtained at autopsy
137 from CJD patients after receiving written informed consent for research use. The
138 diagnosis of CJD, histopathological type, and PrP^{Sc} type were confirmed by PrP
139 immunohistochemistry and western blot analysis. The genotype and mutations in the

140 open reading frame of the *PRNP* gene were determined by sequence analysis as
141 described (14). According to the classification by Parchi *et al* (5), the CJD cases had
142 been classified as follows: sCJD-MM1, 18 cases; sCJD-MM1+2C, 9 cases;
143 sCJD-MM2C, 3 cases; sCJD-MM2T, 4 cases; sCJD-MV2, 3 cases; gCJD-V180I, 9
144 cases; gCJD-E200K, 2 cases; and FFI, 5 cases. Detailed clinicopathological features of
145 one sCJD-MM1+2C patient (H186) with neuronal loss of the inferior olivary nucleus
146 have been reported elsewhere (15).

147

148 **Histopathological analysis**

149 Formalin-fixed brain tissues were treated with formic acid (99% for human tissues or
150 60% for mouse tissues) for 1 hour to inactivate the infectivity and embedded in paraffin.
151 The embedded tissues were sectioned at a thickness of 5 μ m. For PrP
152 immunohistochemistry, tissue sections were pretreated by hydrolytic autoclaving (16).
153 The anti-PrP antiserum PrP-N (17) was used as the primary antibody. Goat-anti-rabbit
154 immunoglobulin polyclonal antibody labelled with the peroxidase-conjugated dextran
155 polymer, EnVision⁺ (Dako, Glostrup, Denmark) was used as the secondary antibody.
156 For routine histopathological analysis, the tissue sections were stained with hematoxylin
157 and eosin (H&E). For quantification of neuronal loss in the inferior olivary nucleus, the
158 tissue sections of the medulla were stained by Klüver-Barrera method (18), and the
159 remaining neurons in the right and left inferior olivary nuclei were counted. The number
160 of the remaining neurons was divided by the area of the inferior olivary nucleus that
161 was measured by ImageJ software version 1.52a (<http://rsb.info.nih.gov/ij/>), and
162 neuronal cell density was calculated.

163

164 **PrP^{Sc} purification**

165 PrP^{Sc} was purified from human brains or mouse brains as described (19). Briefly, brain
166 tissues were homogenized in 2 ml of lysis buffer (100 mM Tris-HCl pH 8.0, 10 mM
167 NaCl, 10 mM MgCl₂, 2% Triton X-100, and 25 units/ml DNase I (Takara Bio)) and
168 digested with collagenase (1 mg/200 mg tissue) (FUJIFILM Wako Pure Chemical
169 Corporation, Osaka, Japan) overnight at room temperature. Collagenase digestion
170 disrupts the connective tissue and improves the accessibility of detergents and/or
171 proteinase K to PrP^{Sc} (20). The digested homogenates were ultracentrifuged at 453,000g
172 for 30 min at 4°C, and the pellets were resuspended and sonicated in 870 µl of
173 proteinase K-digestion buffer (100 mM Tris-HCl pH 8.0 and 5% Sarkosyl
174 (Sigma-Aldrich, St. Louis, MO)). The resuspended samples were centrifuged at 1,000g
175 for 3 min to remove the cell debris, and the supernatants (800 µl) were digested with
176 proteinase K (4 µg/200 mg tissue) (FUJIFILM Wako Pure Chemical Corporation) for 1
177 h at 37°C. It has been reported that these conditions for proteinase K-digestion were
178 sufficient for the complete digestion of normal PrP^C, and that higher proteinase K
179 concentrations caused unfavorable degradation of PrP^{Sc} (21). The proteinase K-digested
180 proteins were precipitated by adding 200 µl of 99.5% ethanol and ultracentrifugation at
181 135,000g for 30 min at 4°C. The pellets were resuspended in 400 µl/200 mg tissue of
182 Laemmli's sample buffer (60 mM Tris-HCl pH 6.8, 5% glycerol, 2% SDS, and 0.01%
183 bromophenol blue) and boiled at 100°C for 10 min.

184

185 **Western blotting**

186 Protein samples were subjected to SDS-PAGE using 13.5% Bis-Tris long gels of 15 cm
187 length and western blotting as described (22). The anti-PrP monoclonal antibody 3F4

188 (BioLegend, San Diego, CA) and type 2 PrP^{Sc}-specific anti-PrP polyclonal antibody
189 Tohoku 2 (23) were used as the primary antibodies. The anti-mouse EnVision+ (Dako)
190 and anti-rabbit EnVision+ (Dako) were used as the secondary antibodies. The blots were
191 visualized with Clarity Max Western ECL substrate (Bio-Rad, Hercules, CA), and
192 images were obtained by imaging device ImageQuant LAS 4000 mini (GE Healthcare,
193 Chicago, IL). The signal intensities of the western blots were quantified with
194 ImageQuant TL software version 7.0 (GE Healthcare).

195

196 **Transmission experiments**

197 The production of knock-in mice expressing human PrP with the 129M/M genotype
198 (Ki-Hu129M/M) has been reported previously (22). Knock-in mice expressing human
199 PrP carrying a causative mutation of FFI (aspartic acid to asparagine at codon 178,
200 Ki-HuD178N) were generated as described (24). The codon 129 genotype of the
201 Ki-HuD178N mice was 129M/M. Intracerebral inoculation was performed as described
202 (25). Briefly, 10% brain homogenates were prepared in sterile phosphate-buffered saline
203 using glass homogenizers, and 20 μ l of the homogenates were intracerebrally inoculated
204 into mice. The inoculated mice were sacrificed at a predefined clinical endpoint, or at
205 the time point showing intercurrent illness. One hemisphere of the brain was fixed in
206 10% buffered formalin for histopathological analysis, and the other hemisphere was
207 immediately frozen for biochemical analysis.

208

209 **Statistical analysis**

210 Signal intensities of PrP^{Sc} bands are expressed as mean \pm SEM ($n = 3$). The
211 Kaplan-Meier log-rank test was used to analyze survival data in transmission study. The

212 statistical tests were carried out using the statistical software EZR version 1.36 (26).

213

214 **Results**

215 **Co-existence of neuropathological characteristics of sCJD-MM2T**

216 Neuronal loss in the thalamus and the inferior olivary nucleus of the medulla is a key
217 neuropathological features of sCJD-MM2T and FFI (3, 27). Since thalamic nuclei are
218 also affected in other CJD subgroups (Supplemental Figure S1), we focused on neuronal
219 loss of the inferior olivary nucleus to identify co-existing M2T prion strain. Systematic
220 neuropathological analysis of archived prion disease tissue samples revealed that 3 out
221 of 18 (17%) sCJD-MM1 patients showed neuronal loss of the inferior olivary nucleus,
222 as with sCJD-MM2T or FFI patients (Figure 1). Other neuropathological changes were
223 typical of sCJD-MM1 such as neuronal loss, spongiform changes, gliosis, and diffuse
224 synaptic-type PrP deposition in the cerebral and cerebellar cortices. Neuropathological
225 features of sCJD-MM2C, *e.g.*, confluent vacuoles or perivacuolar PrP deposition, were
226 not observed in these sCJD-MM1 patients. In addition, 3 out of 9 (33%)
227 sCJD-MM1+2C patients also showed neuronal loss of the inferior olivary nucleus
228 (Figure 1).

229 Although the sCJD-MM1 patients with the inferior olivary degeneration
230 showed prolonged duration of illness *i.e.*, duration from onset to death (Table 1), long
231 clinical course was not solely responsible for the inferior olivary degeneration because
232 sCJD-MM1 patients with prolonged clinical course did not always show neuronal loss
233 of the inferior olivary nucleus (Figure 2). Thus, a part of sCJD patients previously
234 diagnosed as MM1 or MM1+2C had neuropathological characteristics of sCJD-MM2T.

235

236 **Co-existence of biochemical features of sCJD-MM2T**

237 To identify co-existing M2T prion strain biochemically, next we performed western blot
238 analysis of proteinase K-resistant PrP^{Sc} in the brain of the sCJD-MM1 patients with the
239 inferior olivary degeneration. Among the three sCJD-MM1 patients with the inferior
240 olivary degeneration, frozen brain tissues from multiple brain regions were available in
241 two patients (H89 and 0303). In both patients, faint type 2 PrP^{Sc} bands (~19 kDa) were
242 visible alongside with type 1 PrP^{Sc} (~21 kDa) at least one brain region in western blot
243 analysis using a conventional anti-PrP antibody 3F4 (Figure 3). By contrast, no type 2
244 PrP^{Sc} band was detected in a typical sCJD-MM1 case lacking the inferior olivary
245 degeneration (Supplementary Figure S2). Moreover, type 2 PrP^{Sc}-specific antibody,
246 Tohoku 2 (23), revealed that small amounts of type 2 PrP^{Sc} were widely distributed
247 throughout the brain except cerebellum in the two sCJD-MM1 patients with the inferior
248 olivary degeneration. Thus, although the previous examination using only a single brain
249 region had shown only type 1 PrP^{Sc}, re-examination using multiple brain regions
250 identified co-existing type 2 PrP^{Sc} in the sCJD patients previously diagnosed as MM1.
251 Therefore, these patients also had biochemical features of sCJD-MM2T in addition to
252 neuropathological characteristics. The sCJD-MM1+2C patients with the inferior olivary
253 degeneration (H186 and I197) had been previously examined biochemically, and both
254 types 1 and 2 PrP^{Sc} were detected in the brain as shown in Figure 4 (15).

255

256 **Co-existence of transmission properties of sCJD-MM2T**

257 To identify co-existing M2T prion strain based on transmission properties, we
258 performed a transmission study using brain homogenates of sCJD-MM1 or -MM1+2C
259 patients with the inferior olivary degeneration. The inocula were prepared from brain

260 regions where both types 1 and 2 PrP^{Sc} co-existed. In the sCJD-MM1+2C patient, more
261 than one brain region was used for inoculum preparation to enhance the chance of
262 detecting concurrent M2T prion strain because M2T and M2C prion strains are
263 indistinguishable by western blot analysis. The brain homogenates were intracerebrally
264 inoculated into knock-in mice expressing human PrP with the 129M/M genotype
265 (Ki-Hu129M/M) or knock-in mice expressing human PrP carrying a causative mutation
266 of FFI (Ki-HuD178N). The transmission patterns of one sCJD-MM1 material (occipital
267 lobe of 0303) and sCJD-MM1+2C materials (thalamus (I197 Th) or a mixture of the
268 hippocampus and parahippocampus of I197 (I197 Hip)) were identical to those of a
269 typical sCJD-MM1 material. Briefly, the mean incubation period (mean±SD) was
270 shorter in Ki-Hu129M/M mice compared with Ki-HuD178N mice (584±3 days vs.
271 789±82 days for sCJD-MM1 (0303), $P < 0.005$; 554±26 days vs. 653±56 days for
272 sCJD-MM1+2C (I197 Th), $P < 0.005$; 597±4 days vs. 703±55 days for sCJD-MM1+2C
273 (I197 Hip), $P < 0.005$) (Figure 5A-D). In addition, the inoculated Ki-Hu129M/M mice
274 produced a large amount of type 1 PrP^{Sc} whereas Ki-HuD178N mice produced faint
275 type 2 PrP^{Sc} (Figure 6A and B). By contrast, the transmission patterns of the other
276 sCJD-MM1 material (thalamus of H89) was quite different from those of typical
277 sCJD-MM1. Briefly, the infectivity was weak regardless of the mouse genotype (Figure
278 5E-G), and the inoculated Ki-Hu129M/M mice produced faint type 1 PrP^{Sc} whereas
279 Ki-HuD178N mice produced di- and monoglycosylated form-dominant type 2 PrP^{Sc}
280 (Figure 6A and B). These transmission properties were similar to those of typical
281 sCJD-MM2T materials.

282

283 **Discussion**

284 Here we identified concurrence of characteristic features of sCJD-MM2T, *e.g.*, neuronal
285 loss of the inferior olivary nucleus of the medulla, type 2 PrP^{Sc} accumulation, and
286 unique transmission properties, in sCJD patients previously diagnosed as MM1. The
287 present study clearly shows that co-occurrence of M1 and M2T sCJD prion strains in
288 the same patient may also occur.

289 The incidence rate of co-occurrence of M1 and M2T prion strains may be
290 relatively high. In the present study, 3 out of 18 sCJD cases previously diagnosed as
291 MM1 had neuropathological characteristics of sCJD-MM2T. Co-existence of more than
292 one prion strain in the same patient accounts for 35% of total sCJD cases (12).
293 Therefore, the present study, together with previous findings, suggests that
294 co-occurrence of multiple prion strains is more common phenomenon than expected.
295 Indeed, concurrence of M2T prion strain was also suggested in sCJD-MM1+2C patients
296 in the present study. Since faint accumulation of PrP^{Sc} and limited pathological changes
297 are characteristics of M2T prion strain (3), co-existence of M2T prion strain might have
298 been overlooked so far. To estimate the exact prevalence of co-occurrence of M2T prion
299 strain, further analysis will be needed in the future with a larger number of patients. For
300 this aim, the examination of neuronal loss of the inferior olivary nucleus can be one of
301 the sensitive method to identify co-existing M2T prion strain.

302 The co-existing M2T prion strain may affect transmission properties of sCJD.
303 We previously reported that co-existing M2C prion strain did not affect transmission
304 properties of M1 prion strain in mice inoculated with brain materials from
305 sCJD-MM/MV1+2C patients (13). This is because the infectivity of M2C prion strain is
306 very low (6, 13). Therefore, one can consider that the risk of transmission of M2C prion
307 strain from sCJD-MM/MV1+2C patients is negligible. By contrast, M2T prion strain

308 has certain infectivity to PrP-humanized mice (7, 28, 29), although its infectivity is
309 lower than that of M1 prion strain. Indeed, in the present study, one out of four inocula
310 prepared from brains in which co-existence of M2T prion strain was
311 neuropathologically suspected showed unique transmission properties resembling those
312 of M2T prion strain. Meanwhile, only transmission properties of M1 prion strain were
313 observed in transmission experiments of the three other inocula, suggesting that the
314 propagation of M2T prion strain might be overwhelmed by the predominant M1 prion
315 strain.

316 The co-existence of M2T prion strain may also affect duration of illness of
317 sCJD patients. In the present study, all sCJD-MM1 patients with the inferior olivary
318 degeneration showed long duration of illness, *i.e.*, duration from onset to death,
319 compared with the pure form of sCJD-MM1. In sCJD-MM/MV1+2C patients,
320 co-existing M2C prion strain can affect the clinical features of patients, and the duration
321 of illness becomes longer with increasing M2C prion strain load (11, 12). The potential
322 influence of co-existing M2T prion strain on the clinical features, together with those on
323 the neuropathological, biochemical, and transmission properties, suggests that sCJD
324 cases with concurrent M2T prion strain should be considered as distinctive entity such
325 as sCJD-MM/MV1+2T or sCJD-MM/MV1+2C+2T. The clinical features of
326 sCJD-MM/MV1+2T or sCJD-MM/MV1+2C+2T need to be clarified in the future with
327 a larger number of patients.

328 In conclusion, co-occurrence of M1 and M2T prion strains is a novel subgroup
329 of sCJD prion strain co-occurrence. The co-existing M2T prion strain is easily and
330 reliably detectable by histopathological analysis of the inferior olivary nucleus of the
331 medulla.

332

333 **Acknowledgements**

334 We thank members of the Creutzfeldt-Jakob Disease Surveillance Committee in Japan,
335 Creutzfeldt-Jakob disease specialists in the prefectures, and Creutzfeldt-Jakob disease
336 patients and families for providing important clinical information. We thank Hiroko
337 Kudo, Miyuki Yamamoto, and Ayumi Yamazaki for their excellent technical assistance,
338 and Brent Bell for critical review of the manuscript.

339

340 **References**

- 341 1. Prusiner SB, Scott MR, DeArmond SJ, Cohen FE: Prion protein biology. *Cell*
342 1998, 93: 337-348.
- 343 2. Colby DW, Prusiner SB: Prions. *Cold Spring Harb Perspect Biol* 2011, 3: a006833.
- 344 3. Parchi P, Giese A, Capellari S, Brown P, Schulz-Schaeffer W, Windl O, Zerr I,
345 Budka H, Kopp N, Piccardo P, Poser S, Rojiani A, Streichemberger N, Julien J,
346 Vital C, Ghetti B, Gambetti P, Kretzschmar H: Classification of sporadic
347 Creutzfeldt-Jakob disease based on molecular and phenotypic analysis of 300
348 subjects. *Ann Neurol* 1999, 46:224-233.
- 349 4. Parchi P, Zou W, Wang W, Brown P, Capellari S, Ghetti B, Kopp N,
350 Schulz-Schaeffer WJ, Kretzschmar HA, Head MW, Ironside JW, Gambetti P, Chen
351 SG: Genetic influence on the structural variations of the abnormal prion protein.
352 *Proc Natl Acad Sci U S A* 2000, 97: 10168-10172.
- 353 5. Parchi P, Strammiello R, Giese A, Kretzschmar H: Phenotypic variability of
354 sporadic human prion disease and its molecular basis: past, present, and future.
355 *Acta Neuropathol* 2011, 121: 91-112.

- 356 6. Bishop MT, Will RG, Manson JC: Defining sporadic Creutzfeldt-Jakob disease
357 strains and their transmission properties. *Proc Natl Acad Sci USA* 2010, 107:
358 12005-12010.
- 359 7. Moda F, Suardi S, Di Fede G, Indaco A, Limido L, Vimercati C, Ruggerone M,
360 Campagnani I, Langeveld J, Terruzzi A, Brambilla A, Zerbi P, Fociani P, Bishop
361 MT, Will RG, Manson JC, Giaccone G, Tagliavini F: MM2-thalamic
362 Creutzfeldt-Jakob disease: neuropathological, biochemical and transmission studies
363 identify a distinctive prion strain. *Brain Pathol* 2012, 22: 662-669.
- 364 8. Puoti G, Giaccone G, Rossi G, Canciani B, Bugiani O, Tagliavini F: Sporadic
365 Creutzfeldt-Jakob disease: co-occurrence of different types of PrP^{Sc} in the same
366 brain. *Neurology* 1999, 53: 2173–2176.
- 367 9. Schoch G, Seeger H, Bogousslavsky J, Tolnay M, Janzer RC, Aguzzi A, Glatzel M:
368 Analysis of prion strains by PrP^{Sc} profiling in sporadic Creutzfeldt-Jakob disease.
369 *PLoS One* 2006, 3: e14.
- 370 10. Uro-Coste E, Cassard H, Simon S, Lugan S, Bilheude JM, Perret-Liaudet A,
371 Ironside JW, Haik S, Basset-Leobon C, Lacroux C, Peoch K, Streichenberger N,
372 Langeveld J, Head MW, Grassi J, Hauw JJ, Schelcher F, Delisle MB, Andréoletti O:
373 Beyond PrPres type 1 / type 2 dichotomy in Creutzfeldt-Jakob disease. *PLoS*
374 *Pathog* 2008, 4: e1000029.
- 375 11. Cali I, Castellani R, Alshekhlee A, Cohen Y, Blevins J, Yuan J, Langeveld JP, Parchi
376 P, Safar JG, Zou WQ, Gambetti P: Co-existence of scrapie prion protein types 1 and
377 2 in sporadic Creutzfeldt-Jakob disease: its effect on the phenotype and prion-type
378 characteristics. *Brain* 2009, 132: 2643–2658.

- 379 12. Parchi P, Strammiello R, Notari S, Giese A, Langeveld JP, Ladogana A. Incidence
380 and spectrum of sporadic Creutzfeldt-Jakob disease variants with mixed phenotype
381 and co-occurrence of PrP^{Sc} types: an updated classification. *Acta Neuropathol* 2009,
382 118: 659–671.
- 383 13. Kobayashi A, Matsuura Y, Iwaki T, Iwasaki Y, Yoshida M, Takahashi H, Murayama
384 S, Takao M, Kato S, Yamada M, Mohri S, Kitamoto T: Sporadic Creutzfeldt-Jakob
385 disease MM1+2C and MM1 are identical in transmission properties. *Brain Pathol*
386 2016, 26: 95-101.
- 387 14. Kitamoto T, Ohta M, Doh-ura K, Hitoshi S, Terao Y, Tateishi J: Novel missense
388 variants of prion protein in Creutzfeldt-Jakob disease or Gerstmann-Sträussler
389 syndrome. *Biochem Biophys Res Commun* 1993, 191: 709-714.
- 390 15. Iwasaki Y, Mori K, Ito M, Mimuro M, Kitamoto T, Yoshida M: An autopsied case
391 of MM1 + MM2-cortical with thalamic-type sporadic Creutzfeldt-Jakob disease
392 presenting with hyperintensities on diffusion-weighted MRI before clinical onset.
393 *Neuropathology* 2017, 37: 78-85.
- 394 16. Kitamoto T, Shin RW, Doh-ura K, Tomokane N, Miyazono M, Muramoto T,
395 Tateishi J: Abnormal isoform of prion proteins accumulates in the synaptic
396 structures of the central nervous system in patients with Creutzfeldt-Jakob disease.
397 *Am J Pathol* 1992, 140: 1285-1294.
- 398 17. Kitamoto T, Muramoto T, Hilbich C, Beyreuther K, Tateishi J: N-terminal sequence
399 of prion protein is also integrated into kuru plaques in patients with
400 Gerstmann-Sträussler syndrome. *Brain Res* 1991, 545: 319-321.
- 401 18. Kluver H, Barrera E: A method for the combined staining of cells and fibers in the
402 nervous system. *J Neuropathol Exp Neurol* 1953, 12: 400-403.

- 403 19. Muneshige Y, Shimazaki T, Qi Z, Isoda N, Sawa H, Aoshima K, Kimura T, Mohri S,
404 Kitamoto T, Kobayashi A: Development of a quick bioassay for the evaluation of
405 transmission properties of acquired prion diseases. *Neurosci Lett* 2018, 668: 43-47.
- 406 20. Grathwohl KU, Horiuchi M, Ishiguro N, Shinagawa M: Improvement of
407 PrP^{Sc}-detection in mouse spleen early at the preclinical stage of scrapie with
408 collagenase-completed tissue homogenization and Sarkosyl-NaCl extraction of
409 PrP^{Sc}. *Arch Virol* 1996, 141: 1863-1874.
- 410 21. Hizume M, Kobayashi A, Teruya K, Ohashi H, Ironside JW, Mohri S, Kitamoto T:
411 Human prion protein (PrP) 219K is converted to PrP^{Sc} but shows heterozygous
412 inhibition in variant Creutzfeldt-Jakob disease infection. *J Biol Chem* 2009, 284:
413 3603-3609.
- 414 22. Asano M, Mohri S, Ironside JW, Ito M, Tamaoki N, Kitamoto T: vCJD prion
415 acquires altered virulence through trans-species infection. *Biochem Biophys Res*
416 *Commun* 2006, 342: 293-299.
- 417 23. Kobayashi A, Sakuma N, Matsuura Y, Mohri S, Aguzzi A, Kitamoto T:
418 Experimental verification of a traceback phenomenon in prion infection. *J Virol*
419 2010, 84: 3230-3238.
- 420 24. Kitamoto T, Nakamura K, Nakao K, Shibuya S, Shin RW, Gondo Y, Katsuki M,
421 Tateishi J: Humanized prion protein knock-in by Cre-induced site-specific
422 recombination in the mouse. *Biochem Biophys Res Commun* 1996, 222: 742-747.
- 423 25. Kitamoto T, Mohri S, Ironside JW, Miyoshi I, Tanaka T, Kitamoto N, Itohara S,
424 Kasai N, Katsuki M, Higuchi J, Muramoto T, Shin RW: Follicular dendritic cell of
425 the knock-in mouse provides a new bioassay for human prions. *Biochem Biophys*
426 *Res Commun* 2002, 294: 280-286.

- 427 26. Kanda Y: Investigation of the freely available easy-to-use software 'EZR' for
428 medical statistics. *Bone Marrow Transplant* 2013, 48: 452-458.
- 429 27. Parchi P, Petersen RB, Chen SG, Autilio-Gambetti L, Capellari S, Monari L,
430 Cortelli P, Montagna P, Lugaresi E, Gambetti P: Molecular pathology of fatal
431 familial insomnia. *Brain Pathol* 1998, 8: 531-537.
- 432 28. Korth C, Kaneko K, Groth D, Heye N, Telling G, Mastrianni J: Abbreviated
433 incubation times for human prions in mice expressing a chimeric mouse-human
434 prion protein transgene. *Proc Natl Acad Sci USA* 2003, 100: 4784-4789.
- 435 29. Taguchi Y, Mohri S, Ironside JW, Muramoto T, Kitamoto T: Humanized knock-in
436 mice expressing chimeric prion protein showed varied susceptibility to different
437 human prions. *Am J Pathol* 2003, 163: 2585-2593.
- 438

439 **Figure legends**

440 **Figure 1 Neuronal loss of the inferior olivary nucleus of the medulla in CJD**
441 **patients.** A portion of sCJD patients previously diagnosed as MM1 (0701, 0303 and
442 H89) or MM1+2C (1301, I197 and H186) showed decreased neuronal cell density, as
443 with sCJD-MM2T patients or FFI patients.

444

445 **Figure 2 Neuronal loss of the inferior olivary nucleus does not depend on the**
446 **duration of illness.** Data are represented as neuronal cell density of the inferior olivary
447 nucleus of sCJD-MM1 patients (y-axis) plotted against the duration of illness (x-axis).

448

449 **Figure 3 Type 2 PrP^{Sc} accumulation in the sCJD-MM1 patients with neuronal**
450 **loss of the inferior olivary nucleus. A and B,** Multiple brain regions of the sCJD-MM1
451 patients were examined by western blot using anti-PrP antibody 3F4 or type 2
452 PrP^{Sc}-specific antibody Tohoku 2. Type 2 PrP^{Sc} was relatively abundant in the occipital
453 lobe (occipital), a mixture of the hippocampus and parahippocampus (hippocampus),
454 and thalamus in one patient (H89) (**A**), while it was prominent only in the occipital lobe
455 in the other patient (0303) (**B**). A brain sample, equivalent to 0.5 mg in wet weight, was
456 loaded in each lane. The mean signal intensities of PrP^{Sc} in type 1 PrP^{Sc} control
457 (sCJD-MM1) and type 2 PrP^{Sc} control (sCJD-MM2T) were assigned as 100/mm² in
458 each experiment using the 3F4 antibody (gray bars) and Tohoku 2 antibody (black bars),
459 respectively. The signal intensities of PrP^{Sc} are expressed as mean \pm SEM ($n = 3$).

460

461 **Figure 4 Type 2 PrP^{Sc} accumulation in the sCJD-MM1+2C patients with**
462 **neuronal loss of the inferior olivary nucleus.** Type 2 PrP^{Sc} was detected in the

463 occipital lobe, hippocampus, and parahippocampus, though it was indistinguishable
464 whether the detected type 2 PrP^{Sc} was M2T prion strain or M2C prion strain. A brain
465 sample, equivalent to 1 mg in wet weight, was loaded in each lane.

466

467 **Figure 5 Kaplan-Meier survival curves after intracerebral inoculation into**
468 **Ki-Hu129M/M mice (129M/M) or Ki-HuD178N mice (D178N).** Transmission
469 patterns of brain materials from the occipital lobe of sCJD-MM1 (0303) (**A**), thalamus
470 of sCJD-MM1+2C (I197 Th) (**B**), and a mixture of hippocampus and parahippocampus
471 of sCJD-MM1+2C (I197 Hip) (**C**) were similar to those of typical sCJD-MM1 (**D**). By
472 contrast, transmission patterns of brain material from the thalamus of sCJD-MM1 (H89)
473 (**E**) were similar to those of typical sCJD-MM2T (**F** and **G**). Data are represented as %
474 of surviving animals (y-axis) plotted against the number of days post inoculation
475 (x-axis). Incubation time in Ki-Hu129M/M mice inoculated with typical sCJD-MM1
476 material has been reported elsewhere (23).

477

478 **Figure 6 Biochemical properties of PrP^{Sc} in the brain of the inoculated**
479 **Ki-Hu129M/M mice (129M/M) or Ki-HuD178N mice (D178N).** **A** and **B**, Western
480 blot analysis of proteinase K-resistant PrP^{Sc} using the anti-PrP antibody 3F4 (short and
481 long exposures) or type 2 PrP^{Sc}-specific antibody Tohoku 2. For sCJD-MM1 (0303),
482 sCJD-MM1+2C (I197 Th) and sCJD-MM1+2C (I197 Hip), the inoculated
483 Ki-Hu129M/M mice produced large amounts of type 1 PrP^{Sc} similar to those of the
484 Ki-Hu129M/M mice inoculated with a typical sCJD-MM1 material (23), and the
485 inoculated Ki-HuD178N mice produced faint type 2 PrP^{Sc} similar to those of the
486 Ki-HuD178N mice inoculated with the typical sCJD-MM1 material. By contrast, for

487 sCJD-MM1 (H89), the inoculated Ki-Hu129M/M mice produced faint type 1 PrP^{Sc}, and
488 the inoculated Ki-HuD178N mice produced di- and monoglycosylated form-dominant
489 type 2 PrP^{Sc}. The glycosylation patterns of PrP^{Sc} in the Ki-HuD178N mice inoculated
490 with the sCJD-MM1 (H89) material (**A**) were identical to those in the Ki-HuD178N
491 mice inoculated with a typical sCJD-MM2T material (**B**). The amount of brain tissue
492 loaded in each lane is indicated beneath the lane.
493

494 **Table 1. Summary of the clinical features**

	sCJD-MM1 (H89)	sCJD-MM1 (0303)	sCJD-MM1 (0701)
Sex	Male	Male	Female
Age at onset (years)	61	63	71
Initial symptoms	Progressive dementia	Progressive dementia	Progressive dementia
Myoclonus (months)*	15	8	3
Akinetic mutism (months)*	29	12 [†]	6
PSWC on EEG (months)*	15	- [‡]	2
Duration (months)	36	24	24

* The duration until the appearance of myoclonus, akinetic mutism, or PSWC from onset.

[†] The patient became bedridden 7 months after the initial symptoms.

[‡] Only a single EEG examination was performed 2 months after the initial symptoms. EEG revealed a short burst of delta waves and slowing of background activities.

495
496
497
498
499
500
501
502
503
504
505
506
507
508
509
510
511
512
513
514
515
516
517
518

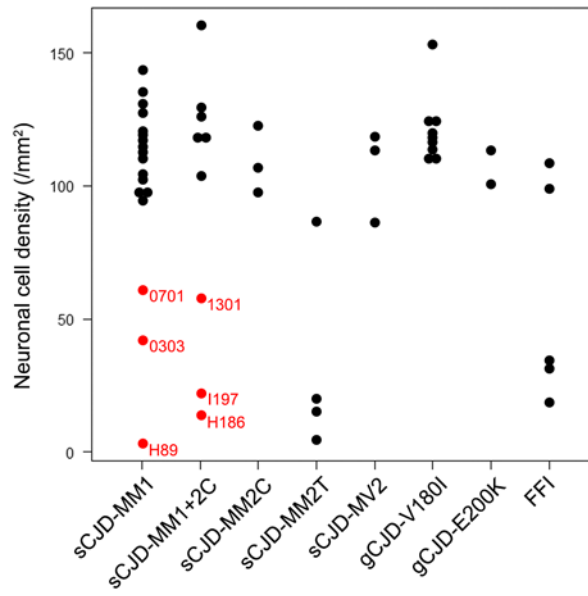


Figure 1

519
520
521
522
523
524
525
526
527
528
529
530
531
532
533
534
535
536
537
538
539
540
541
542

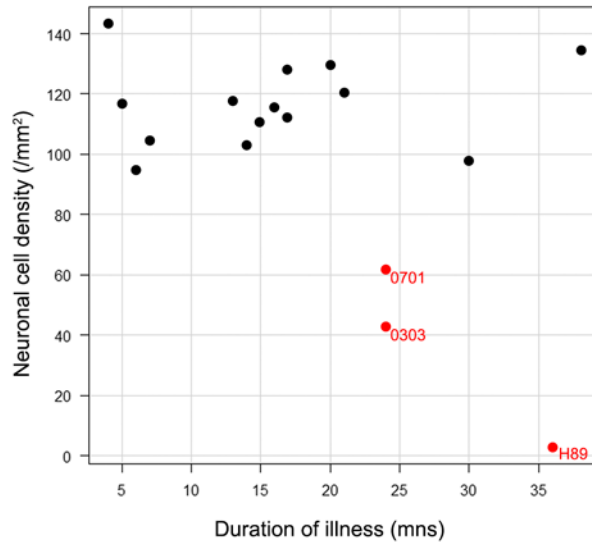
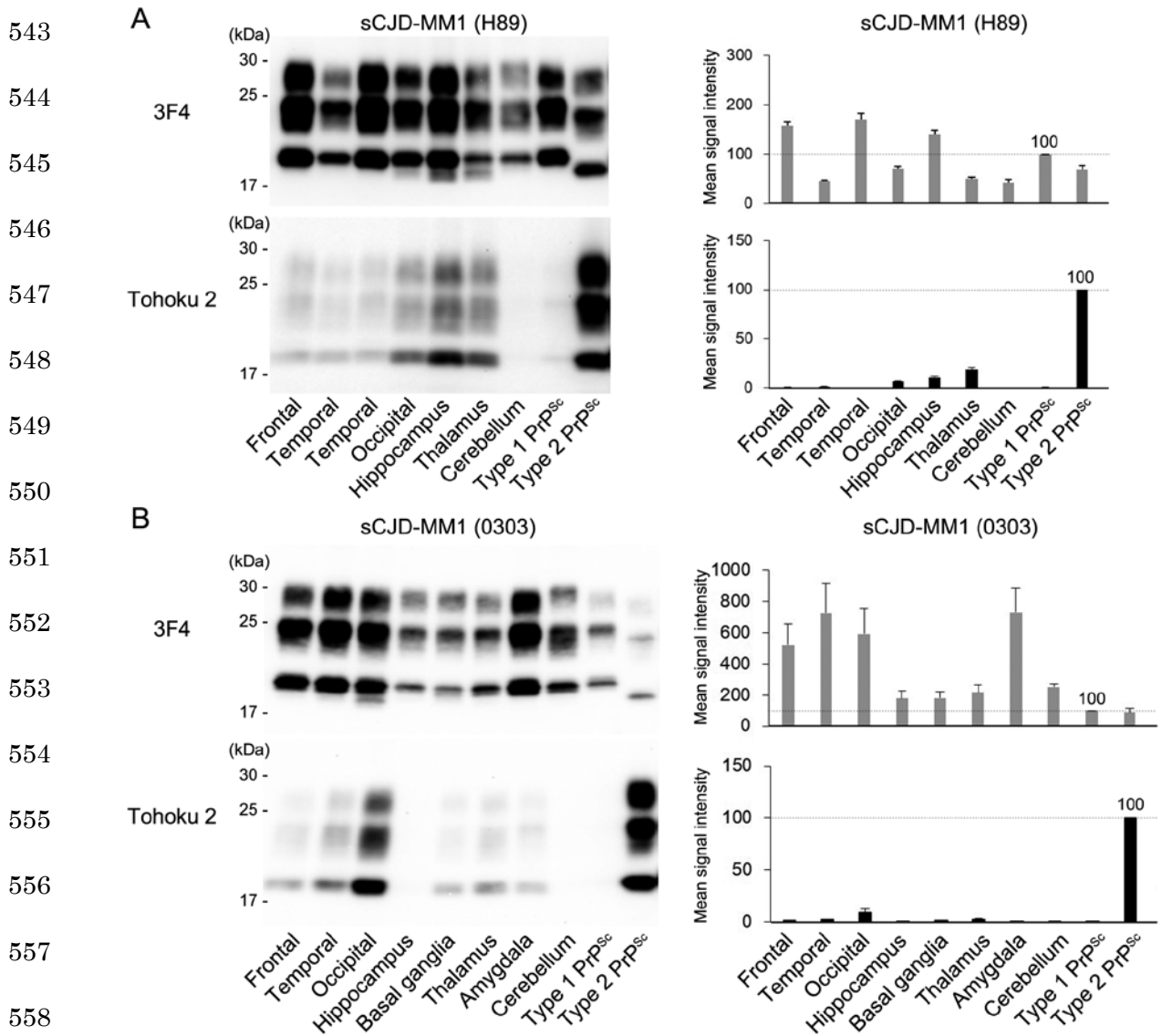


Figure 2



560 Figure 3

567
568
569
570
571
572
573
574
575
576
577
578
579
580
581
582
583
584
585
586
587
588
589
590

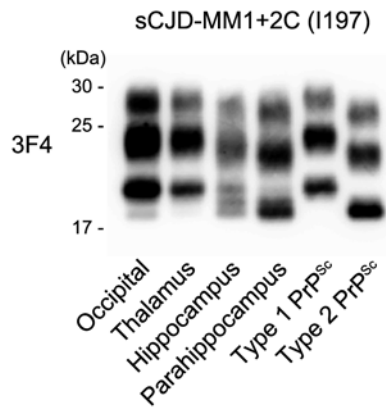


Figure 4

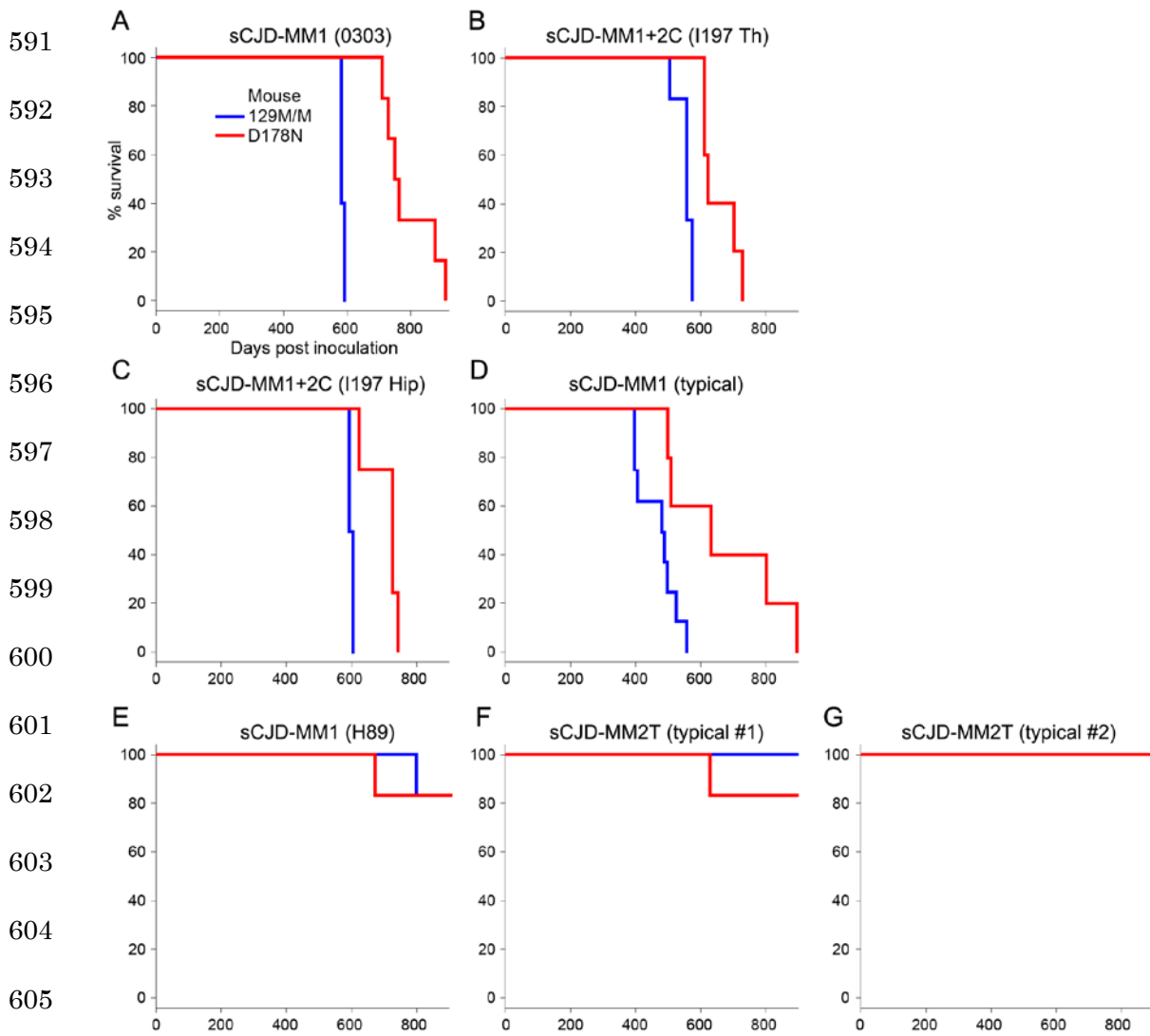


Figure 5

615

A

616

617

618

619

620

621

622

623

624

625

626

627

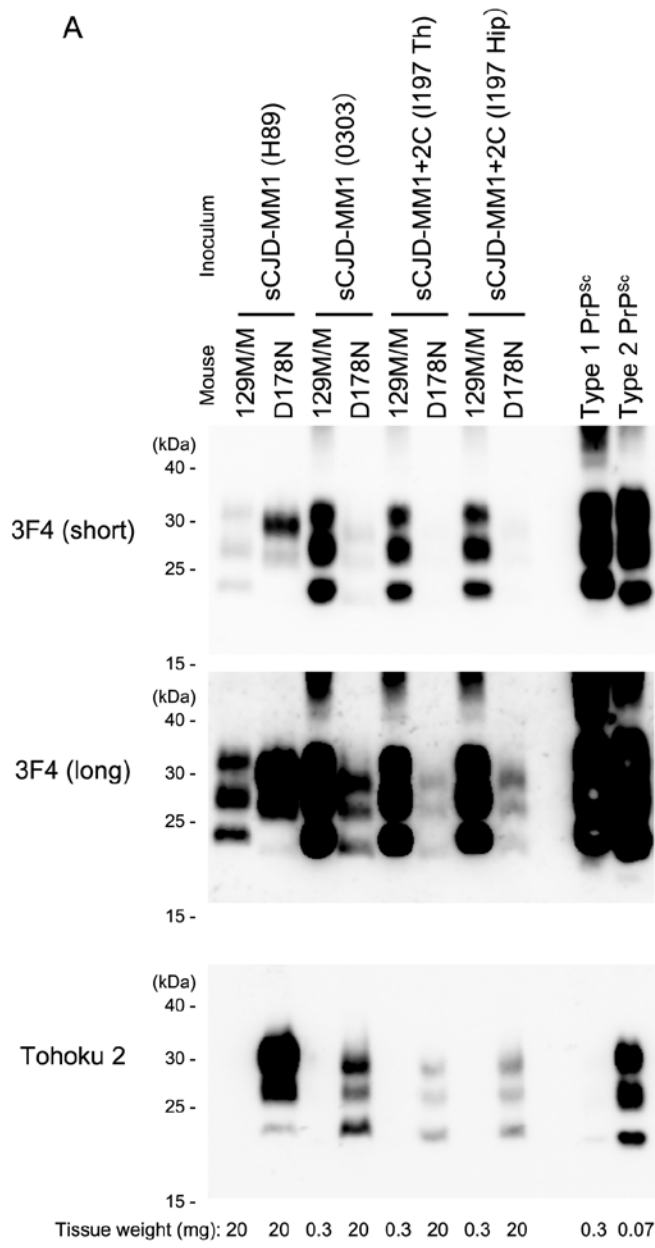
628

629

630

631

632



B

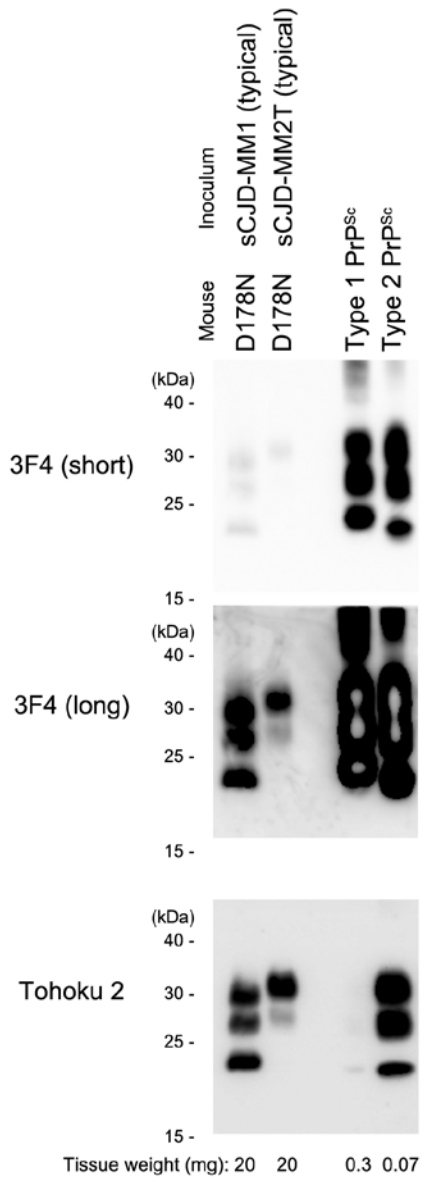


Figure 6

633

634

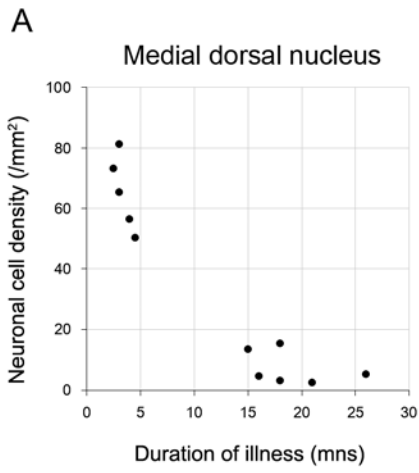
635

636

637

638

639



640

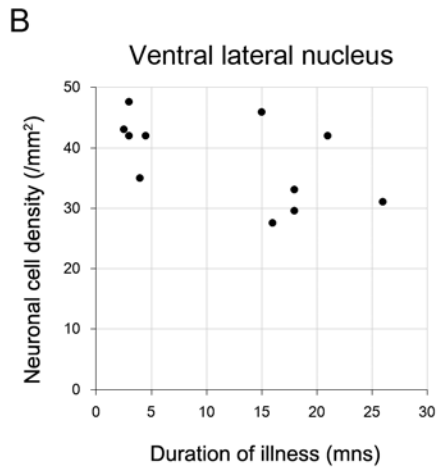
641

642

643

644

645



646

647 Supplemental figure 1

648

649

650

651

652

653

654

655

656

657

658

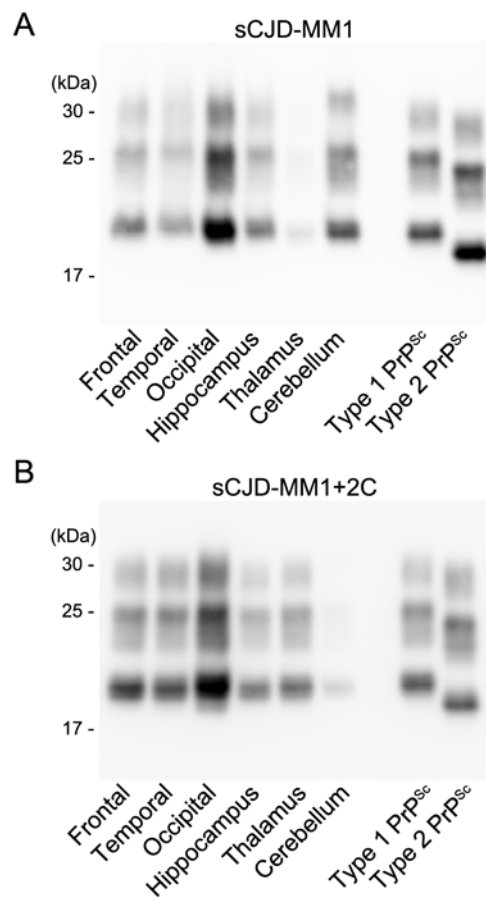
659

660

661

662

663
664
665
666
667
668
669
670
671
672
673
674
675
676
677



Supplemental figure 2

